

Measurement of Υ production with ALICE at LHC: from pp to Pb–Pb collisions

Philippe Rosnet^{1,a} for the ALICE Collaboration

¹LPC, Université Blaise Pascal, CNRS/IN2P3, Clermont-Ferrand, France

Abstract. Quarkonia constitute a sensitive probe of the hot and dense matter created in heavy-ion collisions at high energy. Bottomonium states are particularly interesting because they cannot be produced from the decay of long lived hadrons and their production from statistical hadronization or kinetic regeneration is expected to be marginal. They represent therefore a unique tool to probe the deconfined phase produced in heavy-ion collisions. We present Υ measurements obtained with the ALICE muon spectrometer in pp collisions at $\sqrt{s} = 7$ TeV, in p–Pb collisions at $\sqrt{s_{NN}} = 5.02$ TeV and in Pb–Pb collisions at $\sqrt{s_{NN}} = 2.76$ TeV. Results are obtained in the rapidity range $2.5 < y_{lab} < 4$ and down to zero transverse momentum. They are compared to other LHC data and to model predictions.

1 Introduction

At LHC energies, heavy-quarks Q are produced in initial hard processes, mainly via gluon fusion $gg \rightarrow Q\bar{Q}$. Therefore, quarkonia are formed in the first stage of the collisions and are then sensitive to the subsequent evolution of the Quark-Gluon Plasma (QGP) produced in heavy-ion (A–A) collisions. In the QGP, quarkonium production is expected to be suppressed due to color screening [1]. Since the various quarkonium states have different binding energy, their suppression depends on the temperature of the medium [2]. This makes quarkonium production in heavy-ion collisions a QGP-thermometer. On the other hand, the large production of heavy-quark pairs in high-energy heavy-ion collisions can lead to a statistical regeneration of quarkonia [3, 4]. This effect is however expected to be negligible for bottomonium states, contrarily to charmonium states, because of the much lower production rate of b quarks compared to c quarks [5]. In addition, bottomonium states, unlike charmonium states, cannot be produced from the decays of heavy-flavour hadrons [6].

The interpretation of heavy-ion data requires the comparison with reference pp data, which are not subject to in-medium effects. Quarkonium production in pp collisions is also interesting in itself since it allows to test QCD-based models for the hadro-production mechanism, like the Color Evaporation Model (CEM) [7], the Color-Singlet Model (CSM) [8] and the Non-Relativistic QCD model (NRQCD) [9].

Furthermore, the interpretation of heavy-ion collisions also requires to understand the so-called Cold Nuclear Matter (CNM) effects: shadowing due to modification of the Parton Distribution Func-

^ae-mail: rosnet@in2p3.fr

tions in the nuclei, nuclear dissociation of quarkonia... This is achieved by studying quarkonium production in proton-nucleus (p–A) collisions.

2 Experimental conditions

The ALICE detector [10] is equipped with a muon spectrometer designed to study heavy-flavour and quarkonium production at forward rapidity in the (di)muon channel. High statistics quarkonium measurements are achieved by means of a dedicated dimuon trigger. Other detectors involved are the Silicon Pixel Detector (SPD) of the ALICE central barrel for collision vertex reconstruction, the VZERO scintillators and the Zero-Degree Calorimeter (ZDC) for the measurement of centrality in p–Pb and Pb–Pb collisions. The acceptance of the muon spectrometer for quarkonia is: $p_T > 0$ and $2.5 < y_{\text{lab}} < 4$. The results presented in the following have been obtained from the analysis of pp collisions at $\sqrt{s} = 7$ TeV, p–Pb (and Pb–p) collisions at $\sqrt{s_{NN}} = 5.02$ TeV and Pb–Pb collisions at $\sqrt{s_{NN}} = 2.76$ TeV, corresponding to an integrated luminosity of 1.35 pb^{-1} , 5 nb^{-1} (5.8 nb^{-1}) and $69 \mu\text{b}^{-1}$, respectively.

The performance of the ALICE muon spectrometer to measure Υ 's is illustrated in Fig. 1, which shows the dimuon invariant mass distribution for the integrated pp and Pb–Pb data samples. The Υ mass resolution is about $145 \text{ MeV}/c^2$ in both cases, which allows to separate the three resonant states $\Upsilon(1S)$, $\Upsilon(2S)$ and $\Upsilon(3S)$.

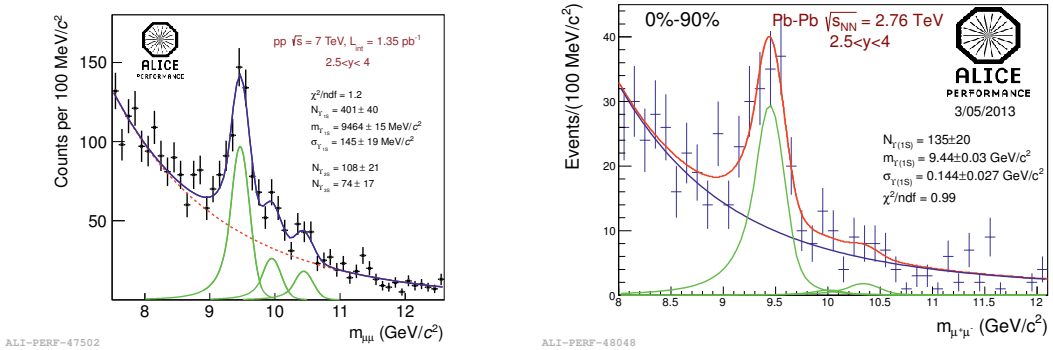


Figure 1. Dimuon invariant mass spectra in the Υ mass region in pp collisions (left) and Pb–Pb collisions (right). The curves correspond to a fit to the data.

3 Proton-proton collisions

3.1 pp results at 7 TeV

The present statistics in the pp data sample allow to perform differential studies for the $\Upsilon(1S)$ only and to measure the integrated cross section of $\Upsilon(2S)$ in the rapidity range $2.5 < y_{\text{lab}} < 4$. The $\Upsilon(3S)$ signal is not significant enough to extract a cross section. Figure 2 shows the Υ production cross sections multiplied by the branching ratios of the dimuon decay channels as a function of rapidity (left) and transverse momentum (right). ALICE data are consistent with results from LHCb [11] which are obtained with about 20 times more integrated luminosity.

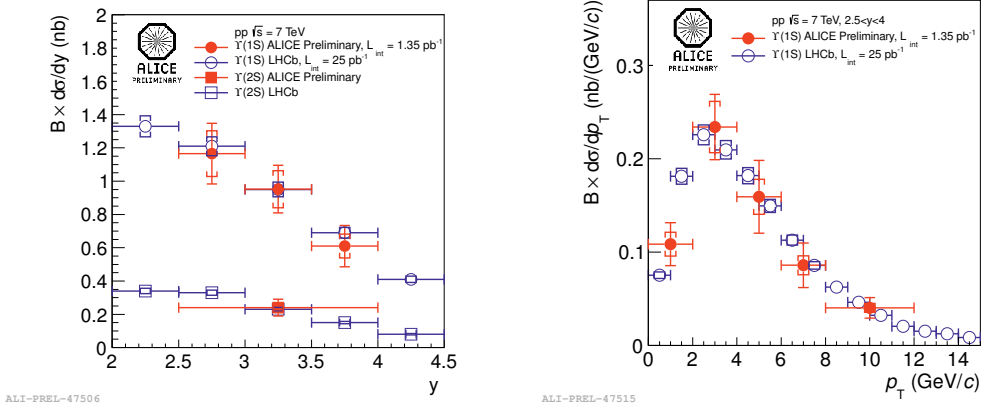


Figure 2. Product of differential cross section times dimuon branching ratio for $\Upsilon(1S)$ and $\Upsilon(2S)$ in pp collisions at $\sqrt{s} = 7$ TeV as a function of rapidity (left) and transverse momentum (right). ALICE data (red points) are compared to LHCb ones (open blue symbols) [11]. Vertical error bars and brackets represent statistical and systematic uncertainties, respectively.

3.2 pp reference at lower energies

The nuclear modification factor R_{AA} (or R_{pA}) is used to quantify the nuclear matter effects in A–A (or p–A) collisions. It is defined as the ratio of the production yield in heavy-ion (or in proton-nucleus) collisions Y_{AA} (or Y_{pA}) and the production cross section in pp collisions σ_{pp} scaled by the average value of the nuclear overlap function $\langle T_{AA} \rangle$ [12]:

$$R_{AA} = \frac{Y_{AA}}{\langle T_{AA} \rangle \sigma_{pp}}.$$

The nuclear modification factor requires the reference pp cross section at the same energy and in the same rapidity range as the one for Pb–Pb and p–Pb data. This is obtained with a two step method: first by interpolating available data at mid-rapidity from Tevatron and LHC to the desired energy, and then, by extrapolating the mid-rapidity result to forward rapidity by using Pythia 6.4 [13] shape with several Parton Distribution Functions. With this method, the pp reference cross sections in the rapidity range $2.5 < y_{lab} < 4$ at $\sqrt{s} = 2.76$ TeV (for Pb–Pb collisions) and at $\sqrt{s} = 5.02$ TeV (for p–Pb collisions) are determined with an accuracy of 15%.

4 In-medium effects

4.1 Pb–Pb results at 2.76 TeV

From the Pb–Pb data sample, 135 $\Upsilon(1S)$ have been extracted while the signal of $\Upsilon(2S)$ and $\Upsilon(3S)$ is not significant. Upsilon production was measured in two rapidity intervals (centrality-integrated) and in two centrality classes (rapidity-integrated): 0–20% most central and 20–90% most peripheral collisions. The nuclear modification factor is presented in Fig. 3. The centrality of the collision is quantified by the average number of participating nucleons $\langle N_{part} \rangle$. This number, as well as $\langle T_{AA} \rangle$, is estimated by using a Glauber model [12].

Figure 3 shows the first observation of $\Upsilon(1S)$ suppression at forward rapidity at LHC energies. The suppression is stronger in the most central collisions where R_{AA} reaches 0.4. If we assume a negligible contribution from regeneration, and since the fraction of $\Upsilon(1S)$ coming from higher resonant states (χ_b , $\Upsilon(2S)$, ...) is about 50% [14], this result is consistent (within uncertainties) with a sequential suppression scenario where all bottomonia except the strongly bound directly produced $\Upsilon(1S)$ are dissolved. The ALICE forward R_{AA} of $\Upsilon(1S)$ as a function of centrality is consistent with the CMS mid-rapidity one [15]. Furthermore, no rapidity dependence of R_{AA} is observed within uncertainties when comparing ALICE to CMS results.

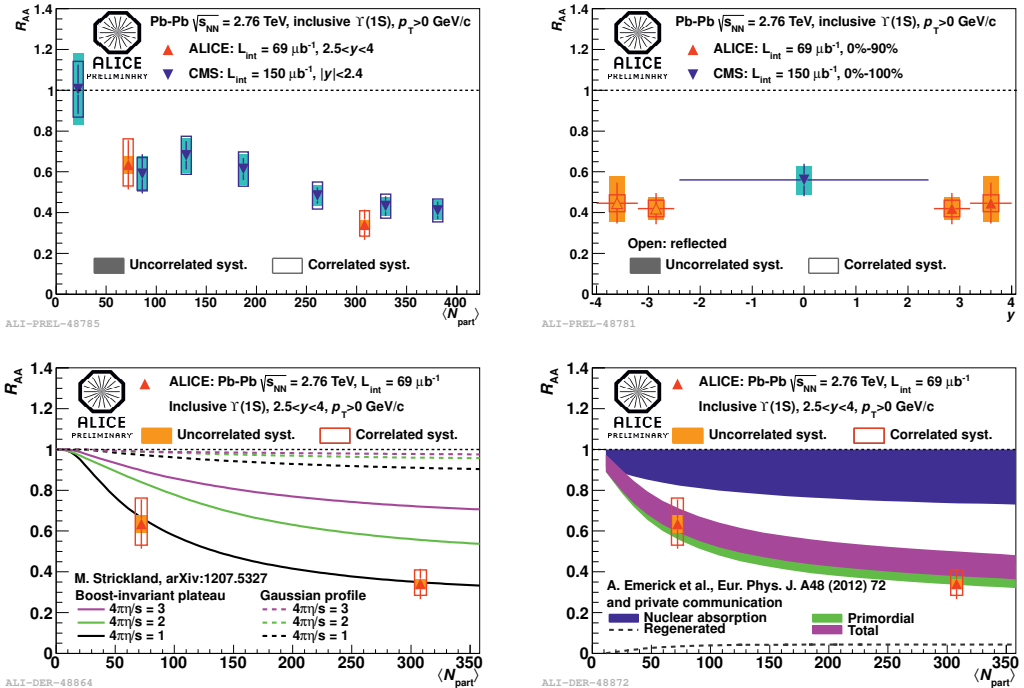


Figure 3. Nuclear modification factor R_{AA} of $\Upsilon(1S)$ in Pb-Pb collisions at $\sqrt{s_{NN}} = 2.76$ TeV as a function of centrality (top left) and rapidity (top right). ALICE forward data (red) are compared to CMS mid-rapidity ones (blue) [15]. Bottom figures show R_{AA} as a function of centrality compared to Strickland model [16] (bottom left) and Emerick et al. model [17] (bottom right). The full and open boxes represent the uncorrelated and the correlated point-to-point systematic uncertainties, respectively. See the text for more details on theoretical predictions.

Results are also compared to theoretical predictions. In Strickland model [16], a complex-valued quarkonium potential is used in an anisotropic hydro-dynamic bulk evolution. In Emerik et al. model [17], Υ production is governed by a kinetic rate equation in an isotropic expanding fireball. Both approaches include feed-down from higher resonant states. In Emerik et al. model, $b\bar{b}$ regeneration is taken into account as well as cold nuclear matter effects, which are parametrized by a nuclear absorption cross section. Figure 3 shows that both models give a fairly good description of the data. Note that in the Strickland model, the amplitude of the suppression is correctly reproduced only in the scenario of a boost invariant plateau temperature (a temperature profile with a large rapidity plateau)

with minimum shear viscosity (in the model, the temperature at $y = 0$ decreases when the shear viscosity increases to match the charged multiplicity $dN_{ch}/dy|_{y=0} \approx 1400$).

4.2 p–Pb results at 5.02 TeV

p–Pb collisions (with the proton beam going in the direction of the muon spectrometer) probe positive rapidity in the nucleon-nucleon centre-of-mass $2.04 < y_{cms} < 3.54$, corresponding to Bjorken variable $x \approx 10^{-4}$ in the nucleus, while Pb–p collisions (with the proton beam going in the opposite direction of the muon spectrometer) probe negative rapidity $-4.46 < y_{cms} < -2.96$, corresponding to $x \approx 0.1$ in the nucleus. The total number of reconstructed $\Upsilon(1S)$ is 280 and 150 for p–Pb and Pb–p collisions, respectively. As for Pb–Pb collisions, only the $\Upsilon(1S)$ study is possible with the present statistics.

The nuclear modification factor R_{pPb} is shown in Fig. 4 (left) as a function of rapidity in the centre-of-mass system. This result reveals a suppression of $\Upsilon(1S)$ in p–Pb collisions, but no clear rapidity dependence is observed within uncertainties. Furthermore, the nuclear modification factor of $\Upsilon(1S)$ is similar to the J/ψ one [18] within uncertainties.

The experimental uncertainties, especially the correlated uncertainties from the pp reference cross section and the estimation of the number of binary collisions, can be reduced by computing the forward-to-backward ratio R_{FB} in the same absolute rapidity range, namely $2.96 < |y_{cms}| < 3.54$:

$$R_{FB}(2.96 < |y_{cms}| < 3.54) = \frac{Y_{p-Pb}(3.43 < y_{lab} < 4)}{Y_{Pb-p}(-3.04 < y_{lab} < -2.5)}.$$

This ratio has the drawback that the statistical uncertainty increases due to the restricted rapidity window. The $\Upsilon(1S)$ R_{FB} is shown in Fig. 4 (right) together with several theoretical predictions.

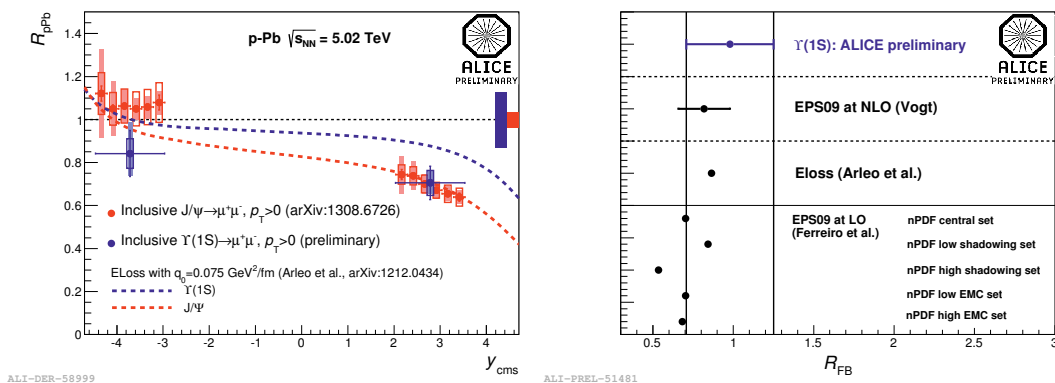


Figure 4. Nuclear modification factor R_{pPb} of $\Upsilon(1S)$ in p–Pb (and Pb–p) collisions at $\sqrt{s_{NN}} = 5.02$ TeV as a function of rapidity in the center-of-mass system (left) and forward-to-backward ratio R_{FB} compared to theoretical predictions (right). On the left, $\Upsilon(1S)$ R_{pPb} (blue points) is compared to J/ψ one (red points) and to the prediction from Arleo et al. (dashed lines). The point-to-point open and full boxes represent the uncorrelated and partially correlated uncertainties, respectively. The fully correlated uncertainty is shown as a blue (red) box for $\Upsilon(1S)$ (J/ψ) around 1 on the right of the figure. See the text for more details on theoretical predictions.

The EPS09 [19] prediction at NLO is based on the CEM approach [20], while the EPS09 prediction at LO is based on the CSM approach [21]. Both predictions are compatible with the ALICE measurement. The EPS09 at LO calculations predict a value which is at the lower edge of the experimental uncertainties, disfavoring a high shadowing effect, and show that the impact of the EMC

effect (depletion of the parton density at $x \approx 0.5$) is negligible. A completely different approach based on coherent parton energy loss in cold nuclear matter [22] is also in good agreement with the measured $\Upsilon(1S)$ forward-to-backward ratio. However, as shown in Fig. 4 (left), the model seems to overestimate slightly the measurement for $\Upsilon(1S)$, both at forward and backward rapidity, even if this disagreement can be explained by the correlated uncertainty.

5 Conclusions

Upsilon production in pp, p–Pb and Pb–Pb collisions has been measured with the ALICE forward muon spectrometer. Results obtained in pp collisions are in good agreement with those from LHCb. The Pb–Pb nuclear modification factor of $\Upsilon(1S)$ indicates a suppression that increases with centrality. This suppression is consistent with the measurement by CMS at mid-rapidity. No evidence of rapidity dependence is observed. The suppression amplitude and shape as a function of centrality is well described by theoretical predictions. The p–Pb data show a small $\Upsilon(1S)$ suppression, possibly increasing from backward to forward rapidity, which indicates that cold nuclear matter effects are not negligible. The comparison of the forward-to-backward ratio with model predictions seems to disfavour a high shadowing effect.

References

- [1] T. Matsui and H.Satz, Phys. Lett. **B 178**, 416 (1986)
- [2] H.Satz, J. Phys. **G 32**, R25 (2006)
- [3] P. Braun-Munzinger and J. Stachel, Phys. Lett. **B 490**, 196 (2000)
- [4] R. L.Thews, M. Schroedter and J. Rafelski, Phys. Rev. **C 65**, 054905 (2001)
- [5] M. Bedjidian et al., arXiv:hep-ph/0311048
- [6] J. Beringer et al. (Particle Data Group), Phys. Rev. **D 86**, 010001 (2012)
- [7] H. Fritzsche, Phys. Lett. **B 67**, 217 (1977)
- [8] R. Baier and R. Rückl Phys. Lett. **B 102**, 364 (1981)
- [9] G. T. Bodwin, E. Braaten and G. L. Lepage, Phys. Rev. **D 51**, 1125 (1995)
- [10] ALICE Collaboration, 2008 JINST **3** S08002
- [11] LHCb Collaboration, Eur. Phys. J. **C 72**, 2025 (2012)
- [12] ALICE Collaboration, Phys. Rev. **C 88**, 044909 (2013)
- [13] T. Sjostrand, S. Mrenna and P. Z. Skands, JHEP **0605**, 026 (2006)
- [14] CDF Collaboration, Phys. Rev. Lett. **84**, 2094 (2000)
- [15] CMS Collaboration, Phys. Rev. Lett. **109**, 222301 (2012)
- [16] M. Strickland, arXiv:1207.5327 [hep-ph]
- [17] A. Emerik, X. Zhao and R. Rapp, Eur. Phys. J. **A 48**, 72 (2012)
- [18] ALICE Collaboration, arXiv:1308.6726 [nucl-ex]
- [19] K. J. Eskola, H. Paukkunen and C. A. Salgado, JHEP **0904**, 065 (2009)
- [20] J. L. Albacete et al., Int. J. Mod. Phys. **E Vol. 22**, 1330007 (2013)
- [21] E. G. Ferreira et al., Eur. Phys. J. **C 73**, 2427 (2013)
- [22] F. Arleo, S. Peigné, arXiv:1212.0434 [hep-ph]